

## 2.6 Deltahedral Zintl Ions of Tin: Synthesis, Structure, and Reactivity

Slavi C. Sevov

Department of Chemistry and Biochemistry, University of Notre Dame, USA

### 2.6.1 Introduction

One little-known area of chemistry is the chemistry of heavy main-group  $p$  elements, mostly metals and semimetals, in negative oxidation states. While the chemistry of  $\text{Sn}^{2+}$  and  $\text{Sn}^{4+}$ , for example, is very well studied and we all learn about it very early in our education, not many people are aware of the fact that tin atoms can accept electrons and exhibit completely different reactivity when negatively charged. For example, catenation and clustering are uncommon for cationic tin, but is the norm for anions, both in inter-metallics and molecular compounds. Thus, cyclopentadienyl-like  $\text{Sn}_5^{6-}$  is found in the inter-metallic compounds  $\text{Na}_8\text{AeSn}_6$  ( $\text{Ae} = \text{Ba}, \text{Eu}$ ),  $\text{Li}_{9-x}\text{AeSn}_{6+x}$  ( $\text{Ae} = \text{Ca}, \text{Eu}$ ),  $\text{Li}_5\text{Ca}_7\text{Sn}_{11}$ , and  $\text{Li}_6\text{Eu}_5\text{Sn}_9$ ,<sup>1</sup> isolated tetrahedra of  $\text{Sn}_4^{4-}$  and alkali-metal cations constitute the structures of  $\text{A}_4\text{Sn}_4$  ( $\text{A} =$  alkali metal),<sup>2</sup> while  $\text{Na}_4\text{CaSn}_6$  and  $\text{Li}_2\text{Ln}_5\text{Sn}_7$  ( $\text{Ln} = \text{Ce}, \text{Pr}, \text{Sm}, \text{Eu}$ ) contain infinite anionic chains and heptane-like  $\text{Sn}_7^{16-}$  oligomers, respectively.<sup>3,4</sup> Notice that, as might be expected, the negative oxidation states are achieved when the more electronegative  $p$  element, tin in this case, is combined with much more electropositive  $s$  or  $f$  element such as the alkali, alkaline-earth, or rare-earth metals. Notice also that, for the purpose of structure rationalization and systematic description, the formal oxidation state assignments assume complete electron transfer from the more electropositive atoms to the  $p$  element. Such polar inter-metallic compounds, called Zintl phases when electronically balanced, are known for all post-transition metals and semimetals.<sup>5</sup>

Negatively charged clusters of some of the  $p$ -metals and semimetals are also stable in solutions and can be crystallized from them as ionic molecular compounds. Known, at present, are a number of such ligand-free anionic clusters, called Zintl ions.<sup>6</sup> Some examples are the clusters with general formulas  $\text{Pn}_7^{3-}$ ,  $\text{E}_9^{3-}$ ,  $\text{E}_9^{4-}$ , and  $\text{E}_5^{2-}$  where  $\text{Pn} = \text{P}, \text{As}, \text{Sb}$  and  $\text{E} = \text{Si}, \text{Ge}, \text{Sn}, \text{Pb}$ . This chapter will limit its attention to the synthesis, structure, and functionalization of molecular anionic clusters of tin. Although both nine- and five-atom clusters are known (Figure 2.6.1), the focus will be predominantly on the nine-atom deltahedral clusters  $\text{Sn}_9^{3-}$  and  $\text{Sn}_9^{4-}$  which are the most readily prepared and most extensively studied species.

### 2.6.2 Background

The history of the Zintl ions starts in 1891 when Joannis experimented with liquid ammonia solutions of sodium and their reactivity towards heavy  $p$ -block elements.<sup>7</sup> He noticed that  $\text{Pb}$  and  $\text{Sb}$  dissolve in such solutions, and the original blue color (due to the solvated free electrons) changed to green for lead and to brown for antimony. Furthermore, he was able to estimate the ratio of  $\text{Na} : \text{Pb}$  as approximately 1 : 2 and this is very close to 4 : 9 (1 : 2.25) of the nowadays well-known clusters  $\text{Pb}_9^{4-}$ . In 1917 this ratio was measured electrolytically more precisely by Smyth and reported as 1 : 2.26.<sup>8</sup> In the meantime, Kraus showed that tin also dissolves in such solutions with a similar color change, this time to red.<sup>9</sup> However, there was no clear understanding of why and under what form these  $p$  elements dissolve. Speculated in some cases was the existence of metal-salt aggregates such as  $\text{Na}_4\text{Sn}\cdot\text{Sn}_8$ ,  $\text{Na}_4\text{Pb}\cdot\text{Pb}_8$ , and  $\text{Na}_3\text{Sb}\cdot\text{Sb}_6$ .

Ten or so years later, in the 1930s, Edward Zintl conducted a series of more systematic studies of these systems.<sup>10</sup> He carried out potentiometric titrations of liquid ammonia solutions of alkali metals with various  $p$  metal salts, typically halides. Thus, the titration of a sodium solution with lead(II) iodide revealed that the green anionic species in solution are  $\text{Pb}_9^{4-}$ . Zintl and coworkers also discovered that

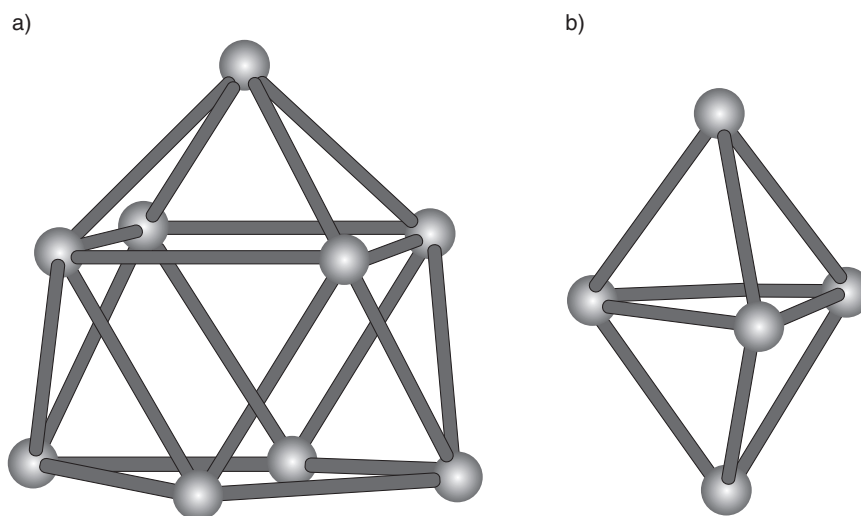


**Figure 2.6.1** The two known anionic clusters of tin: (a) the nine-atom  $\text{Sn}_9^{4-}$  and  $\text{Sn}_9^{3-}$ , and (b) the five-atom  $\text{Sn}_5^{2-}$ . Both clusters are deltahedral, although the nine-atom species has an open square face (the bottom). It is derived from the complete ten-atom deltahedron, a bicapped square antiprism, by removal of one of the capping vertices. The five-atom cluster is a trigonal bipyramid

the same polyatomic anions could be extracted in solutions from binary alloys of the corresponding  $p$  element with an alkali metal mixed in appropriate proportions. Based on these extraction studies they proposed the existence of a number of anions in solution although, at the time, it was assumed that the alloys did not contain these anions, an assumption that was proven wrong more than 65 years later.<sup>11</sup> Some of the proposed species, such as  $\text{E}_9^{4-}$  for  $\text{E} = \text{Sn}, \text{Pb}$  and  $\text{Pn}_7^{3-}$  for  $\text{Pn} = \text{As}, \text{Sb}$ , were structurally characterized later by other groups, while the existence of other proposed species, for example  $\text{Pb}_7^{4-}$ ,  $\text{Bi}_7^{3-}$ ,  $\text{Pn}_5^{3-}$ ,  $\text{Pn}_3^{3-}$  for  $\text{Pn} = \text{As}, \text{Sb}, \text{Bi}$ , was never confirmed.<sup>6</sup> Nonetheless, the recently synthesized mixed-atom clusters  $[\text{Bi}_3\text{M}_2(\text{CO})_6]^{3-}$  ( $\text{M} = \text{Cr}, \text{Mo}$ ),  $[\text{Bi}_3\text{Ni}_4(\text{CO})_6]^{3-}$ ,  $[\text{Sb}_3\text{Ni}_4(\text{CO})_6]^{3-}$ , and  $[\text{Bi}_3\text{Ni}_6(\text{CO})_9]^{3-}$  suggest indirectly that the proposed  $\text{Bi}_3^{3-}$  and  $\text{Sb}_3^{3-}$  may exist in solutions.<sup>12</sup> On the other hand, species like the square-like  $\text{Bi}_4^{2-}$  and the double-bonded oxygen-like  $\text{Bi}_2^{2-}$  were not originally proposed, but have been structurally characterized.<sup>13</sup>

The ions mentioned above and, generally, all polyatomic anions of post-transition metals and semimetals are now known as Zintl ions. Among them, the deltahedral Zintl ions form a special subclass of polyatomic clusters with geometries made of triangular faces. At the time of their discovery, however, the shapes of these anions were unknown. It took more than 30 years after Zintl's work for the first, although partial, structural report to appear. In 1970 Kummer and Diehl reported that, by dissolving an alloy of  $\text{NaSn}_{2.4-2.5}$  in ethylenediamine (= en) they could crystallize a compound with an overall formula  $\text{Na}_4\text{Sn}_9 \cdot 7\text{en}$ .<sup>14</sup> However, it was Corbett who, in 1975, reported the first single-crystal structure with a deltahedral cluster, that of  $\text{Sn}_9^{4-}$  in the compound  $[\text{Na}-(2,2,2\text{-crypt})]_4\text{Sn}_9$ , crystallized by using 2,2,2-crypt (4,7,13,16,21,24-hexaoxa-1,10-diazabicyclo-[8.8.8]-hexacosane) as a sequestering agent of the alkali-metal cations, a method that is now the most common in crystallization of Zintl ions.<sup>15</sup> A year later, Kummer and Diehl reported the structure of  $\text{Na}_4\text{Sn}_9 \cdot 7\text{en}$  with the same  $\text{Sn}_9^{4-}$  deltahedral Zintl ion.<sup>16</sup> Most of the effort during the following 25–30 years was focused primarily on improving

the synthesis and crystallization of Zintl ions, on rationalization of subtle differences in their geometries and electronic structures, and NMR studies of their solutions. In addition to 2,2,2-crypt as a sequestering agent, 18-crown-6 (1,4,7,10,13,16-hexaoxacyclooctadecane) and even smaller crown ethers were found to help crystallization in some cases as well.

The first reaction with deltahedral Zintl ions, which happened to be  $\text{Sn}_9^{4-}$ , was reported in 1988 by Eichhorn, Haushalter, and Pennington.<sup>17</sup> It was a simple ligand exchange reaction in which the labile ligand of a transition-metal complex was replaced by the Zintl ion. Thus,  $\text{Sn}_9^{4-}$  readily replaced the  $\eta^6$ -mesitylene in  $(\text{mes})\text{Cr}(\text{CO})_3$  and formed the corresponding transition-metal complex  $[\text{Sn}_9\text{M}(\text{CO})_3]^{4-}$ .

### 2.6.3 Geometry, Charge, Electron Count, and Electronic Structure

The most stable clusters of tin, as well as of the rest of the elements in this group except carbon, are, by far, the nine-atom clusters. As mentioned above,  $\text{Sn}_9^{4-}$  was the first deltahedral cluster to be structurally characterized. While  $\text{Ge}_9$  was added very soon after,<sup>18</sup> nine-atom clusters of lead and silicon were found respectively 20 and 30 years later.<sup>19,20</sup> Thus, the following discussion of geometry, charges, cluster-bonding, and electronic structure is valid not only for tin clusters, but also for those of silicon, germanium, and lead.

The bonding in the deltahedral clusters cannot be rationalized with simple 2-center–2-electron bonds because it is achieved through delocalized electrons. These clusters are analogous to the well-known cage-like boranes both structurally and electronically, and they similarly follow the Wade–Mingos rules for electron counting.<sup>21</sup> Each BH in the boranes corresponds to a naked atom of group 14 where the B–H bonding pair of electrons is replaced by a lone pair of electrons. For example,  $\text{E}_5^{2-}$  has  $2n + 2 = 12$  cluster bonding electrons (each vertex provides two electrons) as *closo*- $\text{B}_5\text{H}_5^{2-}$ , while  $\text{E}_9^{4-}$  (E = group 14 element) is a *nido*-cluster with  $2n + 4 = 22$  cluster-bonding electrons and corresponds to a *nido*- $\text{B}_9\text{H}_9^{4-}$ .

While experimenting with different synthetic and crystallization techniques for the  $\text{E}_9^{4-}$  clusters, it was discovered that the same clusters, but with a charge of 3–, i.e.  $\text{E}_9^{3-}$ , can be crystallized as well. However, it was not clear what specific conditions lead to one or the other type.  $\text{Sn}_9^{3-}$  was characterized initially in  $[\text{K}-(2,2,2\text{-crypt})]_3\text{Sn}_9 \cdot 1.5\text{en}$  and then in  $[\text{K}-(2,2,2\text{-crypt})]_6(\text{Sn}_9)_2 \cdot 1.5\text{en} \cdot 0.5\text{tol}$  (tol = toluene).<sup>22</sup> The reported compounds with  $\text{Sn}_9^{4-}$ , on the other hand, are many more:  $[\text{Na}-(2,2,2\text{-crypt})]_4\text{Sn}_9$ ,<sup>15</sup>  $\text{Na}_4\text{Sn}_9 \cdot 7\text{en}$ ,<sup>16</sup>  $\text{K}[\text{K}-(2,2,2\text{-crypt})]_3\text{Sn}_9$ ,<sup>23</sup>  $\text{K}[\text{K}-(18\text{-crown-6})]_3\text{Sn}_9 \cdot \text{en}$ ,<sup>24</sup>  $\text{Rb}_2[\text{Rb}-(18\text{-crown-6})]_2\text{Sn}_9 \cdot 1.5\text{en}$ ,<sup>25</sup>  $\text{Cs}_7[\text{K}-(2,2,2\text{-crypt})](\text{Sn}_9)_2 \cdot 3\text{en}$ ,<sup>26</sup>  $[\text{K}-(12\text{-crown-4})]_2[\text{K}-(12\text{-crown-4})]_2\text{Sn}_9 \cdot 4\text{en}$ ,<sup>27</sup> and  $\text{Li}_4\text{Sn}_9 \cdot (\text{NH}_3)_{17}$ .<sup>28</sup> Very similar lists of compounds exist for germanium and lead while for silicon, the cluster with a charge of 4– has not been reported.<sup>6</sup> In addition to the clusters with 3– and 4– charges, a silicon cluster with a charge of 2–, i.e.  $\text{Si}_9^{2-}$ , was also structurally characterized.<sup>29</sup>

Detailed studies carried out for the germanium system revealed that the nine-atom clusters with different charges are in equilibria between themselves and solvated electrons.<sup>30</sup> The same equilibria most likely exist for tin, i.e.  $\text{Sn}_9^{4-}$  and  $\text{Sn}_9^{3-}$  (and possibly  $\text{Sn}_9^{2-}$ ) may coexist in solution in an equilibrium such as  $\text{Sn}_9^{4-} \rightleftharpoons \text{Sn}_9^{3-} + \text{e}^- (\text{solv})$ . It was realized later that the size and the shape of the available counter cations defines which of these species crystallizes from the solutions. Thus, excess of 2,2,2-crypt in solutions with  $\text{K}^+$  leads to the presence of only the very large cations  $[\text{K}-(2,2,2\text{-crypt})]^+$ , and apparently only three such large cations can pack in a crystal lattice with a nine-atom cluster. This means that only  $\text{Sn}_9^{3-}$  clusters can be crystallized in these cases and, indeed, this is observed in  $[\text{K}-(2,2,2\text{-crypt})]_3\text{Sn}_9 \cdot 1.5\text{en}$  and  $[\text{K}-(2,2,2\text{-crypt})]_6(\text{Sn}_9)_2 \cdot 1.5\text{en} \cdot 0.5\text{tol}$ .<sup>22</sup> Deficiency of 2,2,2-crypt, on the other hand, results in the availability of small naked alkali-metal cations. This allows for packing of four cations, some naked and some sequestered, with a cluster anion and this selectively extracts  $\text{Sn}_9^{4-}$  in  $\text{K}[\text{K}-(2,2,2\text{-crypt})]_3\text{Sn}_9$  and

$\text{Cs}_7[\text{K}-(2,2,2\text{-crypt})](\text{Sn}_9)_2 \cdot 3\text{en}$ .<sup>23,26</sup> Apparently, the flat crown ethers have a similar size and shape effect.<sup>24,25,27</sup> In addition, complete absence of a sequestering agent, as in  $\text{Na}_4\text{Sn}_9 \cdot 7\text{en}$  and  $\text{Li}_4\text{Sn}_9 \cdot (\text{NH}_3)_{17}$ , logically leads to the same clusters in the solid state.<sup>16,28</sup> Finally, the crystallization of  $\text{Sn}_9^{4-}$  with  $[\text{Na}-(2,2,2\text{-crypt})]$  maybe due to the smaller size of the sodium cation and its effect on the overall size of the cryptated cation.<sup>15</sup>

Five-atom clusters with a charge of 2− are known for all heavier elements of this group,<sup>20,31</sup> but their synthesis is quite erratic, i.e. there are no clear guidelines for exactly how to crystallize these species. The first  $\text{Sn}_5^{2-}$  clusters, reported by Corbett *et al.*, were crystallized from ethylenediamine solutions of precursors, with nominal compositions anywhere between  $\text{NaSn}$  and  $\text{NaSn}_{1.7}$ .<sup>31a</sup> The same clusters were later crystallized from a solution of a precursor with a nominal composition  $\text{Na}_{1.7}\text{Sn}$ .<sup>31b</sup> Although the nine-atom tin clusters  $\text{Sn}_9^{3-}$  and  $\text{Sn}_9^{4-}$  are typically extracted from similar solutions of precursors with compositions close to  $\text{NaSn}_{2.25}$ , it is not clear how important the different precursor stoichiometries are. Keep in mind that the average charge per tin atom in  $\text{Sn}_5^{2-}$ , 0.4−, is between those of  $\text{Sn}_9^{3-}$ , 0.33−, and  $\text{Sn}_9^{4-}$ , 0.44−, and these numbers do not correlate in any way with the average charge per tin atom in the precursors (assuming complete electron transfer from Na to Sn).

The specific geometry and electronic structure of the nine-atom clusters are very well suited for handling different charges with very small structural distortions and for easy inter-conversion between species with different charges. The overall shape of the clusters can be viewed as that of a tricapped trigonal prism (Figure 2.6.2) in which one, two, or three of the trigonal prismatic edges parallel to the three-fold axis (vertical in Figure 2.6.2) are elongated to some extent.<sup>6a</sup> It has been shown for germanium that lengthening and shortening of these edges involves very little energy, yet greatly affects the electronic structure of the cluster, particularly the energy of the HOMO of the  $\text{E}_9^{4-}$ .<sup>6a</sup> This orbital (Figure 2.6.3) is bonding within the triangular bases of the trigonal prism, but is antibonding between them, most strongly along the same trigonal prismatic edges that change distance. Thus, one or more long edges reduce the antibonding character of the orbital and it is occupied and the HOMO for  $\text{E}_9^{4-}$ , a *nido*-cluster with 22 cluster-bonding electrons. Shortening of the edge(s) pushes the orbital higher in energy because of increasing antibonding character. It becomes occupied by only one electron in  $\text{E}_9^{3-}$ , a radical cluster with 23 cluster-bonding electrons. Further shortening of the edges pushes the orbital even higher in energy, to become empty

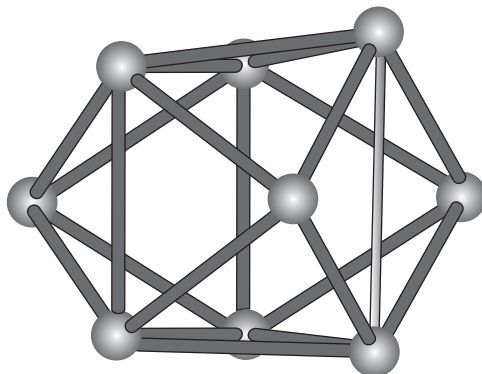


**Figure 2.6.2** The overall shape of a nine-atom cluster viewed as a tricapped trigonal prism (vertical three-fold axis) with one, two, or three elongated trigonal prismatic edges parallel to the three-fold axis. Shown is a cluster with one elongated edge (an open bond), which results in a pseudo-square face. This cluster is identical to the cluster in Figure 2.6.1a, but the pseudo-square face in the latter is at the bottom

## 142 Tin Chemistry: Fundamentals, Frontiers and Applications

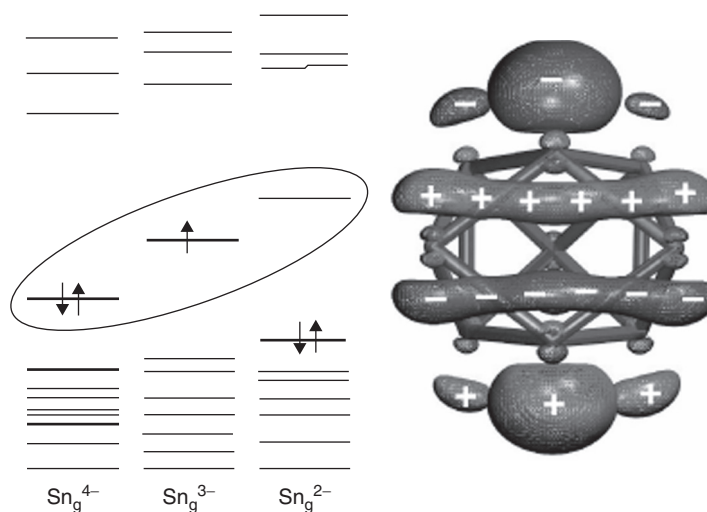


**Figure 2.6.3** Schematic MO diagrams (left) of nine-atom tin clusters with different charges and the frontier orbital (encircled in the MOs and shown to the right) that changes energy upon cluster distortion. This orbital is the HOMO in  $\text{Sn}_9^{4-}$ , the SOMO in  $\text{Sn}_9^{3-}$ , and the LUMO in a hypothetical  $\text{Sn}_9^{2-}$  (known are  $\text{Si}_9^{2-}$  and  $\text{Ge}_9^{2-}$ , although the latter has never been structurally well characterized). Notice that the orbital is  $\pi$ -bonding within the two triangular bases of the trigonal prism (top and bottom triangles), but is  $\sigma$ -antibonding between them along the vertical trigonal prismatic edges. Shortening of the latter increases the antibonding character and pushes the orbital higher in energy as shown

and the LUMO for  $\text{E}_9^{2-}$ , a *closo*-cluster with 20 cluster-bonding electrons. This charge flexibility has been extensively exploited in the case of germanium clusters and it is believed to be responsible for their diverse chemistry of adding a variety of substituents, both nucleophiles and electrophiles.<sup>6a</sup>

Also of interest for later discussion are the three filled orbitals below the HOMO of  $\text{E}_9^{4-}$ . These orbitals are shown in Figure 2.6.4 for a cluster with one elongated edge that generates a pseudo-square open face (the front face in Figure 2.6.4). This face can be capped by an additional vertex, in which case one of

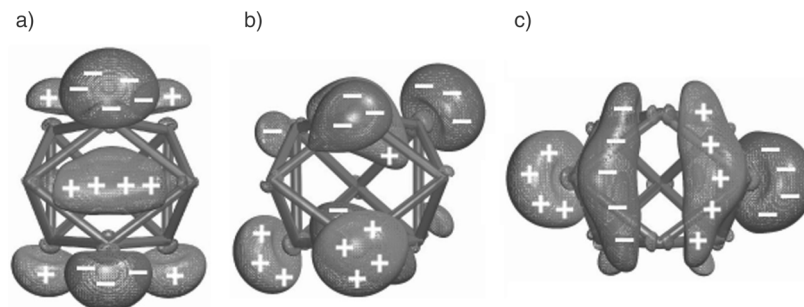


**Figure 2.6.4** The three filled molecular orbitals below the HOMO in  $\text{E}_9^{4-}$  with the cluster shown with its pseudo-square open face in front. If an additional atom is to cap this open face, the MO shown in (a) is perfectly positioned for  $\sigma$ -interactions while those in (b) and (c) can participate in  $\pi$ -interactions

the three orbitals has the appropriate symmetry for  $\sigma$ -overlap (Figure 2.6.4a), while the other two can form  $\pi$ -bonds (vertical and horizontal in Figures 2.6.4b and c, respectively), with suitable orbitals on the capping vertex.

#### 2.6.4 Reactions With Nine-Atom Deltahedral Zintl Anions of Tin

As mentioned already,  $\text{Sn}_9^{4-}$  was the very first deltahedral cluster to undergo a reaction of any kind.<sup>17</sup> The reaction,  $\text{Sn}_9^{4-} + (\text{mes})\text{Cr}(\text{CO})_3 \rightarrow [\text{Sn}_9\text{Cr}(\text{CO})_3]^{4-} + (\text{mes})$ , can be described as a simple ligand exchange reaction in which the cluster replaces a six-electron donating group at the Cr atom and forms  $[\text{Sn}_9\text{Cr}(\text{CO})_3]^{4-}$  (Figure 2.6.5). The  $\text{Cr}(\text{CO})_3$  fragment coordinates at the open pseudo-square face of the  $\text{Sn}_9^{4-}$  cluster. Its three frontier and empty  $d$  orbitals  $z^2$ ,  $xz$ , and  $yz$  are perfectly positioned to interact with the three filled cluster orbitals shown in Figure 2.6.4 resulting in a  $\sigma$ -interaction between  $z^2$  and the orbital in Figure 2.6.4a, and  $\pi$ -interactions between  $xz$  and  $yz$  on  $\text{Cr}(\text{CO})_3$  and the MOs shown in Figures 2.6.4b and c. Therefore, the cluster behaves as a six-electron donating ligand such as mesitylene, benzene, etc. Focusing on the organometallic part of the anion, these six additional electrons are needed to completing the 18-electron environment at the Cr atom. From cluster perspective, on the other hand, this reaction can be viewed as adding the missing vertex in the *nido*- $\text{Sn}_9^{4-}$  to form the corresponding *closo*-species  $[\text{Sn}_9\text{Cr}(\text{CO})_3]^{4-}$ . The latter has the classical shape for a *closo*-cluster with ten vertices, namely a bicapped square antiprism, where chromium is one of the two capping atoms. The fragment  $\text{Cr}(\text{CO})_3$  is isolobal with  $\text{CH}^{3+}$  and, therefore, has three empty frontier orbitals and donates zero electrons to the cluster bonding. This means that the capped cluster retains the original 22 cluster-bonding electrons and, with its ten vertices, corresponds to a *closo*-species according to Wade–Mingos rules.<sup>21</sup> Notice that, overall, the original cluster does not undergo a redox process, it just adds a vertex without loss or gain of electrons.

It was shown later that similar reactions can be carried out with the heavier congeners in the Cr group, Mo and W. It is now known that both  $\text{Sn}_9^{4-}$  and  $\text{Pb}_9^{4-}$  can be derivatized with  $\text{M}(\text{CO})_3$  where  $\text{M} = \text{Cr}$ , Mo, or W to form bicapped square antiprisms where the transition metal caps one of the squares.<sup>17,32–35</sup> (It is somewhat surprising that no analogous  $[\text{Ge}_9\text{M}(\text{CO})_3]^{4-}$  clusters have been characterized to date,

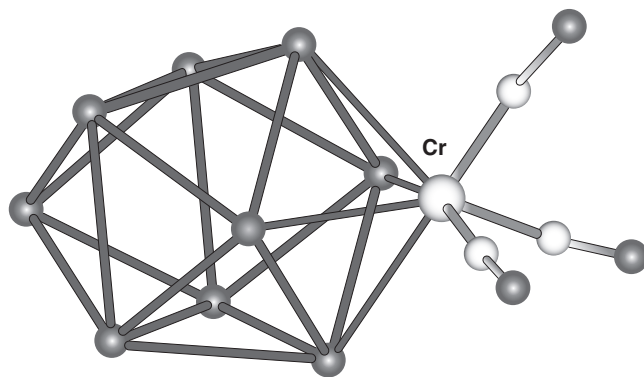


**Figure 2.6.5**  $[\text{Sn}_9\text{Cr}(\text{CO})_3]^{4-}$ , the first derivative of a deltahedral Zintl anion. The  $\text{Cr}(\text{CO})_3$  fragment caps the open pseudo-square face of the original  $\text{Sn}_9^{4-}$  cluster and does not donate electrons for cluster bonding. The hetero-atomic cluster is a *closo*-species according to both shape, a bicapped square antiprism, and electron count. The three empty  $d$  orbitals  $z^2$ ,  $xz$ , and  $yz$  of  $\text{Cr}(\text{CO})_3$  overlap with the filled orbitals shown in Figure 2.6.4 and, therefore, the cluster behaves as a six-electron donating ligand

## 144 Tin Chemistry: Fundamentals, Frontiers and Applications

presumably due to subtle differences in the sizes and electronic properties of the clusters.) However, more recent reports suggest that both  $[\text{Sn}_9\text{M}(\text{CO})_3]^{4-}$  and  $[\text{Pb}_9\text{M}(\text{CO})_3]^{4-}$  may be fluxional in solution (below) with the possibility of the  $\text{M}(\text{CO})_3$  occupying other positions in the cluster.<sup>33–35</sup> Rotation of a triangular face of the cluster was suggested as a possible mechanism for such fluxionality, although such a process would be very complex and involve a series of steps, each associated with a bond cleavage or bond creation. It was later structurally proved that another isomer indeed exists for both tin and lead. The transition metal in the new isomers,  $\eta^5\text{-}[\text{Sn}_9\text{M}(\text{CO})_3]^{4-}$  and  $\eta^5\text{-}[\text{Pb}_9\text{M}(\text{CO})_3]^{4-}$ , occupies a position in the square antiprism and is five-coordinate (Figure 2.6.6).<sup>33,35</sup> Apparently the two tin isomers,  $\eta^4\text{-}[\text{Sn}_9\text{W}(\text{CO})_3]^{4-}$  and  $\eta^5\text{-}[\text{Sn}_9\text{W}(\text{CO})_3]^{4-}$ , cocrystallize from the reaction with  $\text{W}(\text{CO})_3(\text{mes})$ . On the other hand, only  $\eta^4\text{-}[\text{Pb}_9\text{Mo}(\text{CO})_3]^{4-}$  is made by the reaction with the corresponding  $\text{Mo}(\text{CO})_3(\text{mes})$ , while  $\eta^5\text{-}[\text{Pb}_9\text{Mo}(\text{CO})_3]^{4-}$  is produced exclusively from the reaction with  $\text{Mo}(\text{CO})_3(\text{MeCN})$ .<sup>35</sup>

Another report of NMR studies in solutions, however, questions whether the two isomers inter-convert from one to another in solution (dynamic model) or are formed irreversibly during the synthesis (static model).<sup>34</sup> Let us look more closely at these isomers and try to rationalize some possible mechanisms. As already discussed, the open pseudo-square face of these clusters is the most electron-rich place in the free cluster, and it is logical to assume that strong electrophiles, such as  $\text{M}(\text{CO})_3$  will coordinate there (Figure 2.6.7). At this point the new intermediate can undergo two different distortions. The lower energy path is to optimize its geometry by perfecting the two capped faces to squares via further elongation of the former long trigonal prismatic edge and shortening of the other two edges, as shown in Figure 2.6.7b. The resulting cluster is the much more common isomer  $\eta^4\text{-}[\text{E}_9\text{M}(\text{CO})_3]^{4-}$  (Figure 2.6.7c). The second choice for the capped cluster is to undergo a more energy-demanding rearrangement that involves at least one diamond–square–diamond (DSD) transformation (Figure 2.6.7d). This involves breaking the bond between atoms 5–9, as numbered in Figure 2.6.7d, and creating a new bond between the transition metal M and atom 6. A potential second DSD may be occurring at the face made of atoms 1–2–5–6. However,

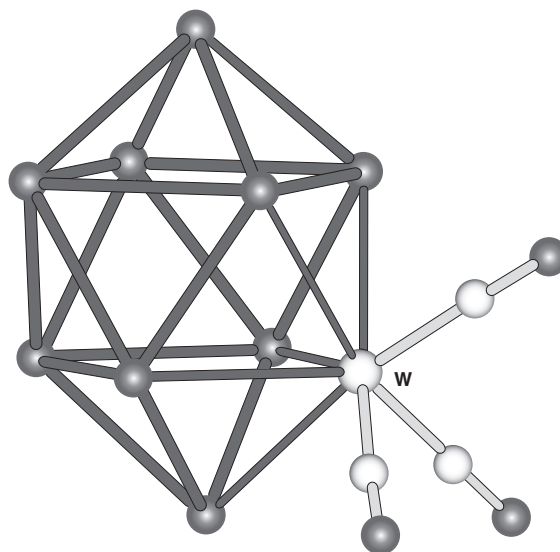


**Figure 2.6.6** The isomer  $\eta^5\text{-}[\text{Sn}_9\text{W}(\text{CO})_3]^{4-}$ , a bicapped square antiprism (the pseudo four-fold axis is vertical), where the transition metal is a part of the square prism and is five-coordinate with the cluster

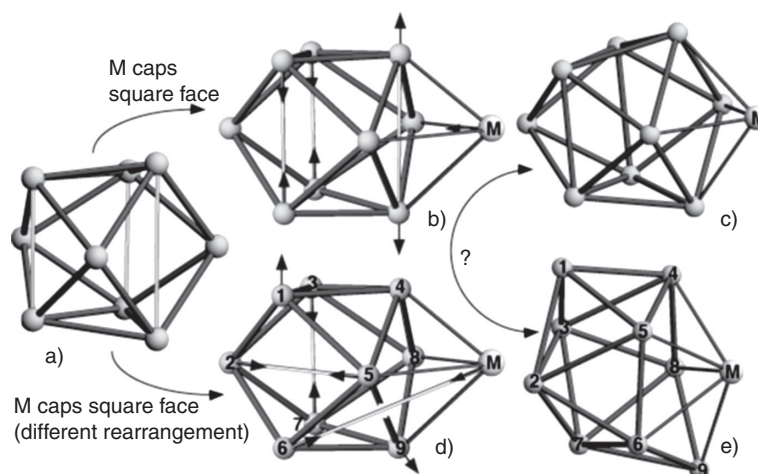


**Figure 2.6.7** Proposed mechanisms for: (a)→(b)→(c) the formation of the more common isomer  $\eta^4$ - $[\text{Sn}_9\text{M}(\text{CO})_3]^{4-}$  and (a)→(d)→(e) the more exotic isomer  $\eta^5$ - $[\text{Sn}_9\text{M}(\text{CO})_3]^{4-}$

as already discussed, the nine-atom clusters may have one, two, or three elongated prismatic edges, and therefore atoms 1–6 may already be far apart.

The described rearrangement followed by geometry optimization would produce the more exotic isomer  $\eta^5$ - $[\text{E}_9\text{M}(\text{CO})_3]^{4-}$  (Figure 2.6.7e). This proposed mechanism is consistent with both the dynamic and static models, i.e. it allows for inter-conversion and equilibrium between the two isomers via the same two intermediates as shown with a question mark in Figure 2.6.7.

In addition to the tricarbonyl fragments, tin clusters can also be capped by ZnPh to form  $[\text{Sn}_9\text{ZnPh}]^{3-}$  (Figure 2.6.8).<sup>36</sup> The reaction is carried out with  $\text{ZnPh}_2$ , and the fragment caps the cluster at the same open pseudo-square face. However, unlike the zero-electron donating tricarbonyl fragments, ZnPh is isolobal with  $\text{CH}_2^+$  and donates one electron to the cluster. This results in a lower charge for the resulting species,

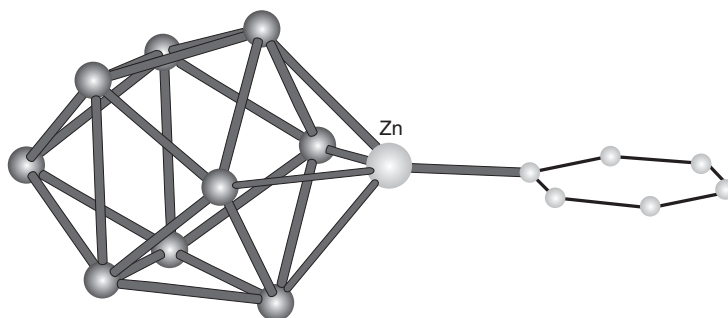


**Figure 2.6.8** The ZnPh-capped cluster  $[\text{E}_9\text{ZnPh}]^{3-}$  for  $\text{E} = \text{Si}, \text{Ge}, \text{Sn},$  and  $\text{Pb}$  made by reaction of the clusters with  $\text{ZnPh}_2$ . The ZnPh fragment is a one-electron donor and reduces the charge of the cluster by one, compared to clusters capped with  $\text{M}(\text{CO})_3$ . The ZnPh fragment is also an electrophile and caps the same open pseudo-square face as  $\text{M}(\text{CO})_3$



i.e. 3– instead of 4–, although the number of cluster-bonding electrons remains 22. There is, however, an example of a capped germanium cluster with 21 bonding electrons,  $[\text{Ge}_9\text{Ni}(\text{CO})]^{3-}$ , where the capping Ni(CO) fragment is a zero-electron donor.<sup>37</sup> It suggests that not only  $\text{E}_9^{4-}$  clusters can be capped, but also those with a lower charge,  $\text{E}_9^{3-}$ .

Besides capping with organometallic fragments, the nine-atom deltahedral clusters can undergo a second type of modification, namely insertion of a transition-metal atom inside the cluster. For example, reactions of  $\text{Pb}_9^{4-}$  with  $\text{Pt}(\text{PPh}_3)_4$  and  $\text{Ni}(\text{COD})_2$  ( $\text{COD} = 1,5\text{-cyclooctadiene}$ ) produce Pt-centered icosahedra  $[\text{Pt}@\text{Pb}_{12}]^{2-}$  and Ni-centered bicapped square antiprisms  $[\text{Ni}@\text{Pb}_{10}]^{2-}$ , respectively.<sup>38</sup> Clearly, the nine-atom clusters have somehow reassembled into 12- and 10-atom species. This behavior, however, seems to be specific only to lead clusters. Thus, similar reactions of  $\text{Ge}_9^{n-}$  clusters with  $\text{Ni}(\text{COD})_2$  produce  $[\text{Ni}@\text{Ge}_9]^{3-}$ , which is a centered version of the empty  $\text{Ge}_9^{3-}$  species.<sup>39</sup> It should be pointed out that the inserted atoms of this group, i.e. Ni, Pd, and Pt, have a closed-shell  $d^{10}$  configuration and do not contribute electrons for cluster-bonding. However, they provide orbitals that overlap with the cluster-bonding orbitals and thus contribute to the overall bonding within the cluster. Although similar centered single-cluster species of tin have not been structurally characterized yet, there is a very good proof that such insertion of a transition-metal atom occurs for them as well. Thus, reaction of tin clusters with  $\text{Ni}(\text{COD})_2$  produces a dimer of Ni-centered  $\text{Sn}_9$  clusters fused via a common vertex.<sup>40</sup> The anion  $[\text{Ni}_2\text{Sn}_{17}]^{4-}$  (Figure 2.6.9) is made of two tricapped trigonal prisms of tin, each of the kind with two elongated prismatic edges (shown lighter in Figure 2.6.9). The two clusters share the tin atom that caps the trigonal prismatic faces with the elongated edges and are positioned at  $90^\circ$  with respect to each other. As shown in Figure 2.6.9, the left prism has its pseudo three-fold axis vertical, while the one to the right has its axis along the viewing direction.

Finally, the nine-atom tin clusters can undergo a third type of modification which is a combination of the two types already discussed, i.e. insertion of a transition-metal atom combined with capping by a fragment of a transition-metal complex. The insertion of the transition metal is most likely the first step of this process. This has been demonstrated for germanium clusters, where the reaction was carried out stepwise by first inserting an Ni atom and then using the product for capping with a NiCO fragment.<sup>37</sup> The inserted transition metal appears to affect the overall electronic structure of the cluster in a subtle way that seems to change the cluster site for preferred coordination of capping fragments, from an open

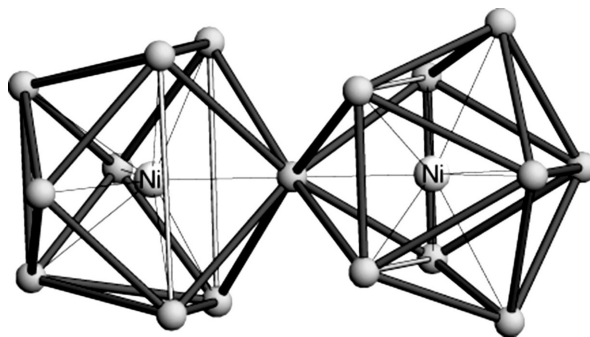


**Figure 2.6.9** The dimer  $[\text{Ni}_2\text{Sn}_{17}]^{4-}$  made of two Ni-centered clusters fused via a common tin vertex. Each half is a tricapped trigonal prism with two elongated prismatic edges (shown lighter), and the common vertex is the atom capping the prismatic face with two elongated edges in each half. The two clusters are rotated around the Ni—Sn—Ni axis by  $90^\circ$  with respect to each other, so that the pseudo three-fold axis of the cluster to the left is vertical, while it is along the viewing direction for the cluster to the right

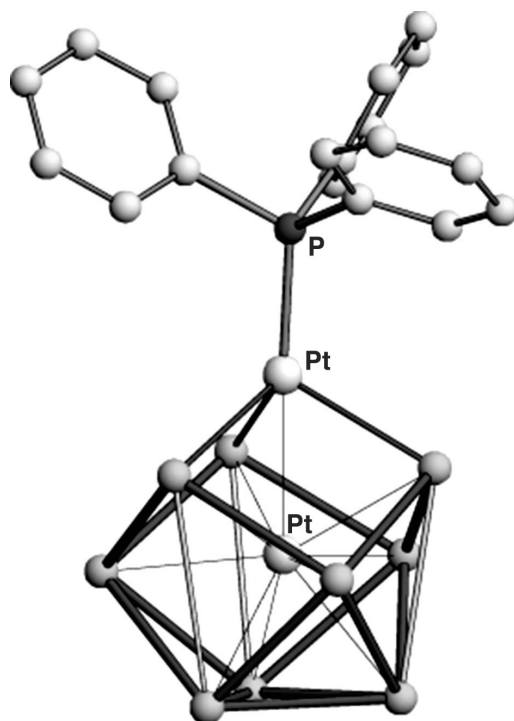


**Figure 2.6.10** The Pt-centered and Pt(PPh<sub>3</sub>)-capped [Pt@(Sn<sub>9</sub>Pt-PPh<sub>3</sub>)]<sup>2-</sup>. The Sn<sub>9</sub> cluster, a tricapped trigonal prism (vertical pseudo three-fold axis), with three elongated edges (shown lighter), is capped at the upper trigonal prismatic base. The capped base opens up as the capping Pt-atom is pressed towards the center of the cluster. The final geometry is very close to spherical, i.e. all atoms, including the capping Pt atom, are at similar distances to the central atom

pseudo-square face to one of the triangular bases of the tricapped trigonal prism. This is observed for all centered and capped germanium clusters [Ni@(Ge<sub>9</sub>Ni-PPh<sub>3</sub>)]<sup>2-</sup>,<sup>41</sup> [Ni@(Ge<sub>9</sub>Ni-CO)]<sup>2-</sup>,<sup>37</sup> [Ni@(Ge<sub>9</sub>Ni-C≡CPh)]<sup>3-</sup>,<sup>37</sup> [Ni@(Ge<sub>9</sub>Ni-en)]<sup>3-</sup>,<sup>37</sup> and the dimer [(Ni@Ge<sub>9</sub>)Ni(Ni@Ge<sub>9</sub>)]<sup>4-</sup>,<sup>39</sup> as well as for one of the two known capped and centered tin clusters, [Pt@(Sn<sub>9</sub>Pt-PPh<sub>3</sub>)]<sup>2-</sup> (Figure 2.6.10).<sup>42</sup> The capping atom in these clusters is apparently pulled towards the center of the cluster, perhaps by interactions with the central atom, to a distance from the center that is similar to those of the nine tin atoms (Figure 2.6.11a, b). This distortion, in turn, causes the capped triangular base to open so much that the corresponding three atoms are no longer in contact with each other (Figure 2.6.11c). The resulting cluster is nearly spherical, with all atoms, including the capping atom, at similar distances from the center. The range of such distances in [Pt@(Sn<sub>9</sub>Pt-PPh<sub>3</sub>)]<sup>2-</sup> is very narrow, 2.70–2.80 Å.<sup>42</sup>

Electronically, the centered and capped clusters are very similar to the empty clusters and can handle different numbers of cluster-bonding electrons, perhaps by small changes in their geometry. They seem to be most stable with 20 cluster-bonding electrons, a number that corresponds to a capped *closo*-species, according to the Wade–Mingos rules, which prescribe  $2n$  electrons for such cases. The number of vertices  $n$  in [M@(E<sub>9</sub>M-L)]<sup>2-</sup> is 10 and the 20 electrons are provided by the nine atoms of group 14 and the charge of 2-. It should be pointed out that despite its higher charge [Ni@(Ge<sub>9</sub>Ni-C≡CPh)]<sup>3-</sup> has the

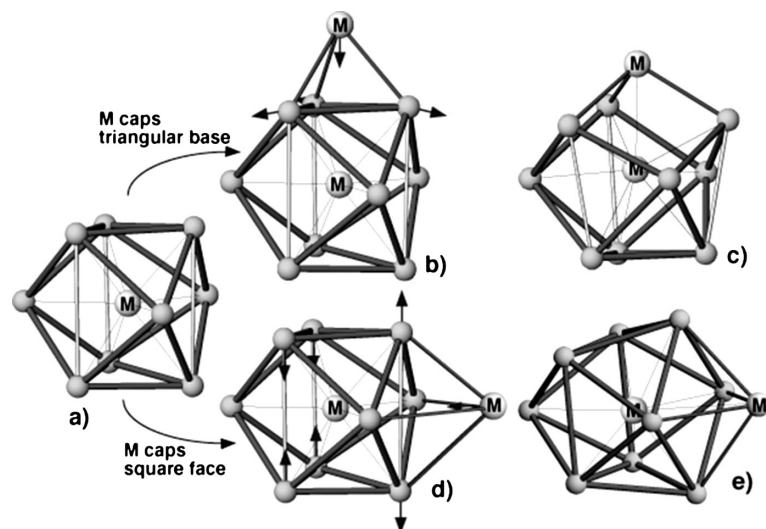


**Figure 2.6.11** The two types of capping observed for centered tin clusters: the path (a)→(b)→(c) represents capping of a triangular base of the tricapped trigonal prismatic cluster; the path (a)→(d)→(e) represents capping of the open pseudo-square face of the cluster as observed also for empty clusters (Figure 2.6.7). The capped triangular base in (b) opens up upon insertion of the capping atom towards the center of the cluster, in order to interact with the central atom, and this results in the cluster shown in (c)

same electron count, simply because the one extra negative charge is for the anionic ligand  $[\text{C}\equiv\text{CPh}]^-$ .<sup>37</sup> There are, however, two examples of centered and capped clusters that carry 21 electrons,  $[\text{Ni}@\text{(Ge}_9\text{Ni-en)}]^{3-}$  and  $[\text{Ni}@\text{(Sn}_9\text{Ni-CO)}]^{3-}$ .<sup>37,42</sup> Again, they should be viewed as derivatives of the corresponding empty  $\text{E}_9^{3-}$  clusters. While the germanium product conforms to the common geometry described above and shown in Figure 2.6.10, the tin species represents the first and only centered cluster that is capped at the open pseudo-square face, as are the empty clusters (Figure 2.6.12). With just this one example it is difficult to even speculate about the reasons for the different geometry in this case. The formation of the species again most likely starts with insertion of the centering atom followed by capping of the face and pulling in the capping atom by interactions with the central atom (Figure 2.6.11a, d, e). The final geometry is not as spherical as for the species with a capped triangular face because the tin atom opposite the capping Ni atom is further out, at 2.83 Å from the center, than the rest of the atoms with distances in the range 2.62–2.68 Å.<sup>42</sup>

### 2.6.5 Solution Studies by NMR

The first extensive NMR studies of deltahedral Zintl ions were carried out by Rudolph and coworkers.<sup>43</sup> Using  $^{117}\text{Sn}$ ,  $^{119}\text{Sn}$ , and  $^{207}\text{Pb}$  NMR they were the first to show that the homo- and hetero-atomic nine-atom deltahedral clusters  $\text{Sn}_9$ ,  $\text{Pb}_9$ ,  $\text{Sn}_{9-x}\text{Ge}_x$ , and  $\text{Sn}_{9-x}\text{Pb}_x$  are fluxional in solution. The homo-atomic clusters exhibit single resonances while multiple signals were observed for the hetero-atomic species due to their different stoichiometries, with one signal per stoichiometry. In addition to this, all the clusters show single spin–spin couplings of the types  $^{117}\text{Sn}$ – $^{119}\text{Sn}$ ,  $^{117}\text{Sn}$ – $^{207}\text{Pb}$ , and  $^{119}\text{Sn}$ – $^{207}\text{Pb}$ . These observations indicate that, on the NMR timescale, all atoms of the cluster are equivalent by dynamic and

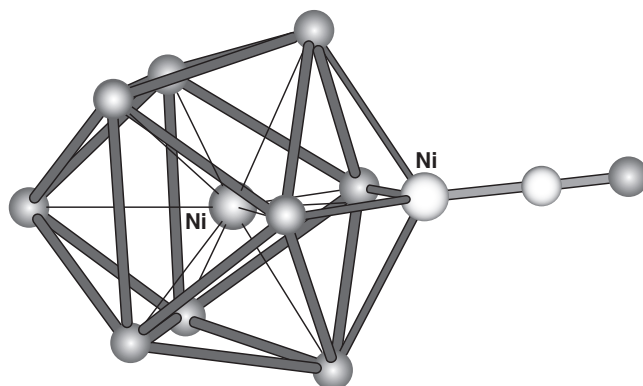


**Figure 2.6.12** The Ni-centered and Ni(CO)-capped cluster  $[\text{Ni}@\text{Sn}_9\text{Ni}(\text{CO})]^{3-}$ , where the open pseudo-square face of the cluster is capped, as in capped empty clusters (Figures 2.6.5 and 2.6.8). This is the only centered and capped cluster with this geometry, all others have the triangular base of the tricapped trigonal prism capped, as in Figure 2.6.10

fast intra-molecular exchange at room temperature. The absence of a signal for  $\text{Sn}_9^{3-}$  can be understood in light of its unpaired electron and paramagnetic character, which will broaden and greatly shift the eventual resonance.

Rudolph and coworkers were also the first to explore reactions of nine atom clusters with transition-metal complexes by NMR, specifically reactions of  $\text{Sn}_9$  and  $\text{Pb}_9$  clusters with  $\text{Pt}(\text{PPh}_3)_4$ .<sup>44</sup> The  $^{119}\text{Sn}$  and  $^{207}\text{Pb}$  NMR experiments again showed single resonances for the corresponding derivatives, in addition to signals from unreacted  $\text{E}_9$  clusters. According to the authors, the observed spin–spin couplings between the cluster and  $^{195}\text{Pt}$  suggested a single platinum atom per cluster. Almost 20 years later the product of this reaction with tin clusters was structurally characterized as  $[\text{Pt}@\text{Sn}_9\text{Pt}(\text{PPh}_3)]^{2-}$  (discussed above, Figure 2.6.10).<sup>42</sup> It was confirmed that in solution the tin atoms are in dynamic exchange while the  $\text{Pt}–\text{Pt}–\text{PPh}_3$  fragment stays rigid, almost like a molten tin drop on a stick. According to the  $^{195}\text{Pt}$  NMR, spin–spin coupling between Sn and Pt occurs only with the central platinum atom and this is consistent with the earlier observations for only one Pt atom per cluster, based on  $^{119}\text{Sn}$  NMR alone.<sup>42</sup>

Finally, two recent NMR studies of the  $\text{W}(\text{CO})_3$  capped tin cluster  $[\text{Sn}_9\text{W}(\text{CO})_3]^{4-}$  (discussed above, Figures 2.6.5 and 2.6.6) suggest different behavior for these species.<sup>33,34</sup> While Eichhorn *et al.* imply dynamic behavior and therefore equilibrium between clusters with differently positioned  $\text{W}(\text{CO})_3$ , i.e. between  $\eta^4$  and  $\eta^5$  coordination,<sup>33</sup> the report by Schrobilgen *et al.* claims that such an interpretation is misleading, due to poor resolution of the NMR spectra.<sup>34</sup> The latter group presents both  $^{117}\text{Sn}$  and  $^{119}\text{Sn}$  NMR spectra that show three different environments for the tin atoms and match the theoretically calculated ones for a static cluster. Similar spectra were observed for the analogous tin clusters capped with  $\text{Cr}(\text{CO})_3$  and  $\text{Mo}(\text{CO})_3$ .<sup>34</sup> The same authors, on the other hand, acknowledge possible dynamic behavior for the  $\text{Mo}(\text{CO})_3$ -capped lead cluster  $[\text{Pb}_9\text{Mo}(\text{CO})_3]^{4-}$ , and migration of the  $\text{Mo}(\text{CO})_3$  from the  $\eta^4$  to the  $\eta^5$  position.<sup>34</sup> This was later confirmed by the structural characterization of  $\eta^5$ - $[\text{Pb}_9\text{Mo}(\text{CO})_3]^{4-}$  made by reaction of lead clusters with  $\text{Mo}(\text{CO})_3(\text{MeCN})$ .<sup>35</sup> Obviously more studies are needed in order to resolve the dispute. One strong piece of evidence in support of the exchange theory is the structurally characterized  $\eta^5$ - $[\text{Sn}_9\text{W}(\text{CO})_3]^{4-}$  coexisting with  $\eta^4$ - $[\text{Sn}_9\text{W}(\text{CO})_3]^{4-}$  in the reaction product.<sup>33</sup>

### 2.6.6 Concluding Remarks

The nine-atom deltahedral Zintl ions of group 14 are fascinating species in many respects: unusual bonding, aesthetically pleasing and yet flexible geometry, and very rich chemistry. The observed reactivity of the tin clusters with transition-metal compounds is similar to that of germanium clusters and this suggests that many more similarities may be expected between the two systems. The chemistry of the germanium clusters has been much more extensively studied at this stage.<sup>6a</sup> It has been shown that they participate in additional reactions such as oligo- and polymerization, functionalization with main-group organometallic fragments ( $\text{SnR}_3$ ,  $\text{GeR}_3$ ,  $\text{SbR}_2$ ,  $\text{BiR}_2$ ) and with various organic groups, addition of alkenes by reactions with alkynes, etc. All this indicates that similar reactions with tin clusters may result in the corresponding functionalized tin analogs or, perhaps, even unexpected and potentially more interesting species.

### Acknowledgments

I would like to thank my former and current coworkers Angel Ugrinov, Jose Goicoechea, Michael Hull, and Donald Chapman for their many discoveries in the chemistry of the Zintl ions. The financial support by the National Science Foundation (CHE-0446131 and CHE-0742365) is greatly appreciated.

### References

1. (a) Todorov, I. and Sevov, S. C., *Inorg. Chem.* **2004**, *43*, 6490; (b) Todorov, I. and Sevov, S. C., *Inorg. Chem.* **2005**, *44*, 5361.
2. Schäfer, H. and Eismann, B., *Rev. Mat. Sci.* **1985**, *15*, 1.
3. Todorov, I. and Sevov, S. C., *Inorg. Chem.* **2006**, *45*, 4478.
4. Todorov, I. and Sevov, S. C., *Inorg. Chem.* **2007**, *46*, 4044.
5. (a) Sevov, S. C. in *Intermetallic Compounds Principles and Practice: Progress*, Eds. J. H. Westbrook and R. L. Fleischer, John Wiley & Sons, Ltd., Chichester, England, **2002**, pp. 113–132; (b) *Chemistry, Structure, and Bonding of Zintl Phases and Ions*, Ed. S. M. Kauzlarich, VCH Publishers, Inc., New York, NY, **1996**; (c) Pottgen, R., *Z. Naturforsch.* **2006**, *61*, 677.
6. Recent reviews: (a) Sevov, S. C. and Goicoechea, J. M., *Organometallics* **2006**, *25*, 567; (b) Fässler, T. F., *Coord. Chem. Rev.* **2001**, *215*, 377; (c) Corbett, J. D., *Angew. Chem. Int. Ed.* **2000**, *39*, 670; (d) Corbett, J. D., *Chem. Rev.* **1985**, *85*, 383; (e) Corbett, J. D., *Struct. Bonding* **1997**, *87*, 157.
7. (a) Joannis, A., *Hebd. Seances Acad. Sci.* **1891**, *113*, 795; (b) Joannis, A., *Hebd. Seances Acad. Sci.* **1892**, *113*, 587; (c) Joannis, A., *Ann. Chim. Phys* **1906**, *7*, 75.
8. Smyth F. H., *J. Am. Chem. Soc.* **1917**, *39*, 1299.
9. (a) Kraus, C. A., *J. Am. Chem. Soc.* **1907**, *29*, 1571; (b) Kraus, C. A., *J. Am. Chem. Soc.* **1922**, *44*, 1216; (c) Kraus, C. A., *Trans. Am. Electrochem. Soc.* **1924**, *45*, 175; (d) Kraus, C. A., *J. Am. Chem. Soc.* **1925**, *47*, 43.
10. (a) Zintl, E., Goubeau, J. and Dullenkopf, W. *Z. Phys. Chem., Abt. A* **1931**, *154*, 1; (b) Zintl, E. and Harder, A. *Z. Phys. Chem., Abt. A* **1931**, *154*, 47; (c) Zintl, E. and Dullenkopf, W., *Z. Phys. Chem., Abt. B* **1932**, *16*, 183; (d) Zintl, E. and Kaiser, H., *Z. Anorg. Allg. Chem.* **1933**, *211*, 113; (e) Zintl, E., Harder, A., and Neumayr, S., *Z. Phys. Chem., Abt. A* **1931**, *154*, 92.
11. Queneau, V. and Sevov, S. C., *Angew. Chem. Int. Ed. Engl.* **1997**, *36*, 1754.
12. (a) Goicoechea, J. M., Hull, M. W., and Sevov, S. C., *J. Am. Chem. Soc.*, in press; (b) Xu, L., Ugrinov, A., and Sevov, S. C., *J. Am. Chem. Soc.* **2001**, *123*, 4091.
13. (a) Cisar, A. and Corbett, J. D. *Inorg. Chem.* **1977**, *16*, 2482; (b) Xu, L., Bobev, S., El-Bahraoui, J., and Sevov, S. C., *J. Am. Chem. Soc.* **2000**, *122*, 1838.
14. Kummer, D. and Diehl, L. *Angew. Chem., Int. Ed. Engl.* **1970**, *9*, 895.
15. (a) Corbett, J. D. and Edwards, P. A., *J. Chem. Soc., Chem. Commun.* **1975**, 984; (b) Corbett, J. D. and Edwards, P. A., *J. Am. Chem. Soc.* **1977**, *99*, 3313.
16. Diehl, L., Khodadadeh, K., Kummer, D., and Strähle, J., *Chem. Ber.* **1976**, *109*, 3404.

## Deltahedral Zintl Ions of Tin: Synthesis, Structure, and Reactivity 151

17. Eichhorn B. W., Haushalter, R. C., and Pennington, W. T., *J. Am. Chem. Soc.* **1988**, *110*, 8704.
18. Belin, C. H. E., Corbett, J. D., and Cisar, A., *J. Am. Chem. Soc.* **1977**, *99*, 7163.
19. (a) Fässler, T. F. and Hunziker, M., *Inorg. Chem.* **1994**, *33*, 5380; (b) Campbell, J., Dixon, D. A., Mercier, H. P. A., and Schrobilgen, G. J., *Inorg. Chem.* **1995**, *34*, 5798.
20. Goicoechea, J. M. and Sevov, S. C., *J. Am. Chem. Soc.* **2004**, *126*, 6860.
21. (a) Wade, K. J., *Adv. Inorg. Chem. Radiochem.* **1976**, *18*, 1; (b) Wade, K., *J. Chem. Soc. D* **1971**, 792; (c) Mingos, D. M. P., *Nat. Phys. Sci.* **1972**, *99*, 236; (d) Mingos, D. M. P., *Acc. Chem. Res.*, **1984**, *17*, 311.
22. (a) Critchlow, S. C. and Corbett, J. D., *J. Am. Chem. Soc.* **1983**, *105*, 5715; (b) Fässler, T. F. and Hunziker, M., *Z. Anorg. Allg. Chem.* **1996**, *622*, 837.
23. Burns, R. C. and Corbett, J. D., *Inorg. Chem.* **1985**, *24*, 1489.
24. Fässler, T. F. and Hoffmann, R., *Angew. Chem. Int. Ed.* **1999**, *38*, 543.
25. Hauptmann, R. and Fässler, T. F., *Z. Anorg. Allg. Chem.* **2002**, *628*, 1500.
26. Hauptmann, R., Hoffmann, R., and Fässler, T. F., *Z. Anorg. Allg. Chem.* **2001**, *627*, 2220.
27. Ugrinov, A. and Sevov, S. C., *Appl. Organomet. Chem.* **2003**, *17*, 373.
28. Korber, N. and Fleischmann, A., *J. Chem. Soc., Dalton Trans.* **2001**, 383.
29. Goicoechea, J. M. and Sevov, S. C., *Inorg. Chem.* **2005**, *44*, 2654.
30. Ugrinov, A. and Sevov, S. C., *Chem. Eur. J.* **2004**, *10*, 3727.
31. (a) Edwards, P. A. and Corbett, J. D., *Inorg. Chem.* **1977**, *16*, 903; (b) Birchall, T., Burns, R. C., Devereux, L. A., and Schrobilgen, G. J., *Inorg. Chem.* **1985**, *24*, 890; (c) Campbell, J. and Schrobilgen, G. J. *Inorg. Chem.* **1997**, *36*, 4078; (d) Somer, M., Carrillo-Cabrera, W., Peters, E., Peters, K., Kaupp, M., and von Schnering, H. G., *Z. Anorg. Allg. Chem.* **1999**, *625*, 37.
32. Eichhorn, B. W. and Haushalter, R. C., *J. Chem. Soc., Chem. Commun.* **1990**, 937.
33. Kesanli, B., Fettinger, J., and Eichhorn, B. W., *Chem. Eur. J.* **2001**, *7*, 5277.
34. Campbell, J., Mercier, H. P. A., Franke, H., Santry, D. P., Dixon, D. A., and Schrobilgen, G. J. *Inorg. Chem.* **2002**, *41*, 86.
35. Yong, L., Hoffmann, S. D., and Fässler, T. F., *Eur. J. Inorg. Chem.* **2005**, 3663.
36. Goicoechea, J. M. and Sevov, S. C., *Organometallics*, **2006**, *25*, 4530.
37. Goicoechea, J. M. and Sevov, S. C., *J. Am. Chem. Soc.* **2006**, *128*, 4155.
38. (a) Esenturk, E. N., Fettinger, J., Lam, Y.-F., and Eichhorn, B. W. *Angew. Chem. Int. Ed.* **2004**, *43*, 2132; (b) Esenturk, E. N., Fettinger, J., and Eichhorn, B. W., *Chem. Commun.* **2005**, 247.
39. Goicoechea, J. M. and Sevov, S. C., *Angew. Chem. Int. Ed.* **2005**, *44*, 2.
40. Esenturk, E. N., Fettinger, J., and Eichhorn, B. W., *J. Am. Chem. Soc.* **2006**, *128*, 12.
41. (a) Gardner, D. R., Fettinger, J., and Eichhorn, B. W., *Angew. Chem., Int. Ed. Engl.* **1996**, *35*, 2852; (b) Esenturk, E. N., Fettinger, J., and Eichhorn, B. W., *Polyhedron*, **2006**, *25*, 521.
42. Kesanli, B., Fettinger, J., Gardner, D. R., and Eichhorn, B. W., *J. Am. Chem. Soc.* **2002**, *124*, 4779.
43. (a) Rudolph, R. W., Wilson, W. L., Parker, F., Taylor, R. C., and Young, D. C. *J. Am. Chem. Soc.* **1978**, *100*, 4629; (b) Rudolph, R. W., Taylor, R. C., and Young, D. C. *J. Am. Chem. Soc.* **1981**, *103*, 2480; (c) Wilson, W. L., Rudolph, R. W., Lohr, L. L., Taylor, R. C., and Pyykko, P., *Inorg. Chem.* **1986**, *25*, 1535.
44. Teixidor, F., Luetkens, M. L., Jr., and Rudolph, R. W., *J. Am. Chem. Soc.* **1983**, *105*, 149.